FEBS Letters 530 (2002) 24–30 FEBS 26554

Specificity of substrate recognition by type II dehydroquinases as revealed by binding of polyanions[1]

Lewis D.B. Evans[a], Aleksander W. Roszak[a,b], Lorna J. Noble[a,b], David A. Robinson[a,b], Peter A. Chalk[c], Jennifer L. Matthews[a,b], John R. Coggins[a], Nicholas C. Price[a], Adrian J. Lapthorn[b,*]

[a] *Division of Biochemistry and Molecular Biology, Institute of Biomedical and Life Sciences, University of Glasgow, Glasgow G12 8QQ, UK*
[b] *Department of Chemistry, University of Glasgow, Glasgow G12 8QQ, UK*
[c] *GlaxoSmithKline Medicines Research Centre, Gunnels Wood Road, Stevenage SG1 2NY, UK*

Received 29 July 2002; accepted 8 August 2002

First published online 25 September 2002

Edited by Stuart Ferguson

Abstract The interactions between the polyanionic ligands phosphate and sulphate and the type II dehydroquinases from *Streptomyces coelicolor* and *Mycobacterium tuberculosis* have been characterised using a combination of structural and kinetic methods. From both approaches, it is clear that interactions are more complex in the case of the latter enzyme. The data provide new insights into the differences between the two enzymes in terms of substrate recognition and catalytic efficiency and may also explain the relative potencies of rationally designed inhibitors. An improved route to the synthesis of the substrate 3-dehydroquinic acid (dehydroquinate) is described.

Key words: Dehydroquinase; 3-Dehydroquinic acid; Substrate recognition; X-ray crystallography; Phosphate; Sulfate

1. Introduction

Dehydroquinase (3-dehydroquinate dehydratase, EC 4.2.1.10; DHQase) catalyses the reversible dehydration of 3-dehydroquinate to form 3-dehydroshikimate. This reaction is part of two metabolic pathways: the biosynthetic shikimate pathway and the catabolic quinate pathway [1–3]. The biosynthetic pathway leads in a series of seven steps to the formation of chorismate, which is the precursor of a number of aromatic compounds including the amino acids Phe, Tyr and Trp, vitamins E and K, folate and ubiquinone. This pathway has been considered an attractive target for the development of antimetabolites as it is present in bacteria, higher plants, fungi and protozoa, but absent in mammals. In the catabolic pathway, quinate can be converted in three steps to *p*-hydroxybenzoate which can be used as a source of carbon atoms via the β-ketoadipate pathway.

Two distinct types of enzymes have been described with DHQase activity. Type I enzymes, which involve a *syn* elimination reaction, usually catalyse the biosynthetic reaction. By contrast type II enzymes, which can catalyse either the biosynthetic or catabolic reactions, involve an *anti* elimination reaction [2,4]. The two types of DHQases are quite distinct from one another in terms of both amino acid sequences and three-dimensional structures [5]. Type I enzymes are dimers of 27 kDa subunits which contain an $(\alpha/\beta)_8$ fold; by contrast type II enzymes are dodecameric with the 16 kDa subunits arranged as tetramers of trimers. Each type II DHQase subunit adopts a flavodoxin-type fold, consisting of a five-stranded parallel β-sheet core flanked by four α-helices [5]. In terms of catalytic mechanism, type I enzymes are known to proceed via an imine intermediate [6] whereas type II enzymes are believed to involve an enol [7] intermediate. High resolution structural data are available for the type I enzyme from *Salmonella typhi* and for the type II enzymes from *Mycobacterium tuberculosis* and *Streptomyces coelicolor* [5,7].

The type II DHQases which have been kinetically characterised appear to fall into two groups. The enzymes from organisms such as *S. coelicolor* and *Aspergillus nidulans* have high relatively values of k_{cat}, in the range 100–1000 s^{-1} at pH 7.0 and 25°C [2,8]. By contrast the enzymes from *Helicobacter pylori*, *M. tuberculosis* and *Neurospora crassa* have much lower values of k_{cat} in the range 10 s^{-1} or lower [3,9–11]. There appears to be no obvious correlation between the values of k_{cat} and K_m for these enzymes.

In this paper we characterise the interactions between type II DHQases and the polyanionic ligands sulphate and phosphate using a combination of kinetic and structural approaches. Preliminary results [2] had indicated that phosphate behaves as a competitive inhibitor of the type II DHQase from *A. nidulans*, with a K_i of 10 mM at pH 7.0 and 25°C. In the present work we extend these studies to other type II enzymes for both phosphate and sulphate. The X-ray crystallographic data on the enzymes from *S. coelicolor* and *M. tuberculosis* complexed with phosphate and sulphate respectively, identify significant differences in both the mode of binding and number of polyanions bound by the two enzymes. The differences in binding of the anion to the carboxylate recognition site of the enzymes may account for the

*Corresponding author. Fax: (44)-141-330 4888.
E-mail address: adrian@chem.gla.ac.uk (A.J. Lapthorn).

[1] The atomic coordinates have been deposited in the Protein Data Bank with the accession code 1H05.

Abbreviations: MTDHQase, dehydroquinase from *Mycobacterium tuberculosis*; SCDHQase, dehydroquinase from *Streptomyces coelicolor*; HPDHQase, dehydroquinase from *Helicobacter pylori*; TBDMSCl, *t*-butyldimethylsilyl chloride; 4-DMAP, 4-dimethylaminopyridine; DMF, dimethylformamide; PDC, pyridinium dichromate

0014-5793/02/$22.00
PII: S0014-5793(02)03346-X

relative potencies of several rationally designed inhibitors [12]. In addition, the binding of a second anion in the position of the lid domain of the *M. tuberculosis* DHQase structure may help to explain the complex kinetic effects of the polyanions observed for this enzyme.

2. Materials and methods

2.1. Molecular biology and protein purification

The genes encoding the type II DHQases, *aroD* from *M. tuberculosis* and *aroQ* from *H. pylori*, have been cloned previously [9,13]. Both genes were amplified by PCR using plasmid DNA (GlaxoSmithKline) as a template, with the addition of a 5′ *Nde*I restriction site and a 3′ *Bam*HI restriction site. The PCR product was cloned into pT7-Blue-3 (Invitrogen) by blunt-ended ligation and sequencing of double-stranded DNA templates was undertaken by the chain termination method with 'big dye' terminators. The fragments were separated and displayed on an ABI 373 DNA sequencer using ABI Prism software. A 0.5 kb *Nde*I–*Bam*HI fragment containing the gene encoding DHQase was then cloned into pET-15b (Novagen), which encodes an N-terminal 6×His tag, and the resulting plasmids were termed p-MPET and p-HPET respectively. p-MPET and p-HPET were transformed into *Escherichia coli* strain BL21 DE3 (*p-lysS*) for over-expression.

Over-expression and purification of both 6×His-tagged MTDHQase and HPDHQase were carried out in the following manner. *E. coli* cells containing the p-ET-15b-derived plasmids were grown with shaking in 25 ml LB (Sigma) containing 100 μg/ml ampicillin overnight at 37°C. These cultures were used to inoculate 500 ml of LB+100 μg/ml ampicillin and grown with shaking at 37°C until the optical density at 600 nm was between 0.4 and 0.6. Isopropyl-β-D-thiogalactoside (0.8 mM) was added to induce expression of the plasmid and cells grown for 4 h. Cells were harvested by centrifugation (4000×*g*, 20 min) and resuspended in phosphate-buffered saline. Cell pellets were again centrifuged (4000×*g*, 20 min) and stored at −20°C.

Cell pellets were de-frosted and resuspended in 20 mM Tris–HCl (Sigma), 300 mM NaCl (BDH), 20 mM imidazole (Fluka). EDTA-free protease inhibitors (Roche), and DNase I (Sigma) were added and cells were lysed by passage through a French press (2×950 psi). Cell debris was removed by centrifugation (8000×*g*, 60 min) and the supernatant passed through a 20 μm filter and loaded onto a Ni-NTA superflow column (Qiagen). All subsequent manipulations were carried out using an FPLC system (Amersham) at 4°C. The column was washed with buffer A (20 mM Tris–HCl, 300 mM NaCl)+20 mM imidazole until the A_{280} reached the baseline level. Buffer A+75 mM imidazole was then used as a second wash before elution of the 6×His-tagged DHQase from the column with buffer A+200 mM imidazole. Buffer exchange into buffer B (50 mM Tris–HCl, 100 mM NaCl, 1 mM EDTA) was carried out using a pressure cell concentrator (Amicon) and the protein loaded onto a Q-Sepharose column (Amersham) pre-equilibrated with buffer B. The column was washed with buffer B and the protein eluted by a salt gradient from 100 mM to 500 mM NaCl. Purified 6×His-tagged DHQase was stored at 4°C in buffer B, or stored at −20°C in buffer B+50% glycerol. SCDHQase was purified as previously reported [14].

Table 1
Crystallographic and structure determination statistics

Data collection details	
Data set	
MTDHQ+SULPHATE	
Wavelength (Å)	0.870
Detector distance (mm)	180
Space group	F23
Unit cell dimensions ($a=b=c$ in Å)	126.635
Resolution range (Å)	30.0–1.45
Observations	85 115
Unique reflections	24 274
Completeness (highest res. shell)	89.9% (32.7%[a])
R_{merge}[b] (%)	3.9
Refinement statistics	
Resolution range (Å)	30.0–1.5
R-factor[c] (R_{work}/R_{free})	13.9/19.1
Number of atoms[d]	1058/20/200
RMS bond length deviation (Å)	0.025
RMS bond angle deviation (°)	1.0
Mean B-factor (Å)[e]	20/23/30/40
RMS backbone deviation (Å)	1.3
Coordinate error (Å)[f]	0.08

[a]Data were processed to the edge (corners) of the CCD detector leading to a drop in completeness above 1.8 Å resolution (76% complete).
[b]$R_{merge}=\Sigma|I-\langle I\rangle|/\Sigma\langle I\rangle$.
[c]R-factor $=\Sigma|F_o-F_c|/\Sigma F_o$.
[d]Number of atoms of protein, heteroatoms and water molecules respectively.
[e]Mean B-factor for main chain, side chain, inhibitor and water atoms respectively.
[f]Calculated using the method of Cruickshank [24].

2.2. Crystallisation and X-ray data collection

MTDHQase was concentrated to 7 mg/ml using Centricon-30 centrifugal concentrators (Amicon) and crystallisation experiments carried out by sitting-drop vapour diffusion using in-house sparse matrix screens. Crystals of size 0.1×0.1×0.1 mm were obtained in 30% 2-methylpentane-2,4-diol, 0.5 M ammonium sulphate, 0.1 M HEPES, pH 7.5 after several weeks and required no further optimisation. Crystals were frozen to 100 K, using artificial mother liquor as cryoprotectant and X-ray data were collected at synchrotron radiation source Daresbury station 9.6, using the CCD (ADSC) Quantum 4 detector. The crystals diffracted to 1.5 Å and were found to belong to the cubic space group F23, with unit cell dimensions $a=b=c=126.64$ Å, with one monomer in the asymmetric unit. Data were processed and scaled with DENZO and SCALEPACK [15].

2.3. Model building and refinement

The structure of MTDHQase plus sulphate was solved by molecular replacement using the stand-alone version of AMoRe [16] with the apoMTDHQase structure (PDB I.D. 2DHQ) as a search model. A single unambiguous peak (peak height 50% greater than the next highest peak) was found in the rotation function. Correct translation function solutions had correlation coefficients of 54.8% and R-factors of 39%, which were then subjected to rigid body refinement in AMoRe to give a final correlation coefficient of 80.3% and an R-factor of 26.3%. The structure was refined using all data from 30.0 Å to 1.5 Å using REFMAC [17] from the CCP4 suite of programs [18] and manual model building was carried out using QUANTA (Accelrys). The final model statistics are shown in Table 1.

2.4. Synthesis of dehydroquinate

The synthesis used in this work (Scheme 1) is a modification of the published route to (2*R*)-2-bromodehydroquinic acid and (2*R*)-2-fluorodehydroquinic acid [19] and has been carried out successfully on a gram scale. All compounds synthesised gave ^{1}H- and ^{13}C-NMR spectra comparable with published data. Full details of the synthesis are given in the Appendix.

Direct lactonisation of quinic acid (step a) was achieved by heating quinic acid to reflux in acidified benzene using a Dean-Stark apparatus. The secondary hydroxyl was protected (step b) by heating with *t*-butyldimethylsilyl chloride (TBDMSCl) and catalytic 4-dimethylaminopyridine (4-DMAP) in dimethylformamide (DMF), with the 3- and 4-monosilylated products formed in equal amounts and separated by silica gel column chromatography. The unprotected 3-hydroxyl was then oxidised (step c) using pyridinium dichromate (PDC) in the presence of 3 Å molecular sieves, and the desired product was deprotected (step d) by treatment with acetic acid at 50°C.

2.5. Kinetic studies of DHQase

Type II DHQase activity was assayed by monitoring the increase in A_{234} accompanying conversion of 3-dehydroquinate to 3-dehydroshikimate [14]. Assays were performed at 25°C using 50 mM Tris-acetate buffer, pH 7.0 in a total volume of 1 ml. Reactions were initiated by addition of enzyme (0.015 μg, 0.5 μg and 3 μg of SCDHQase, MTDHQase and HPDHQase respectively). Kinetic parameters were obtained by varying substrate concentrations over the appropriate range (between 20 μM and 2 mM) in the presence and absence of

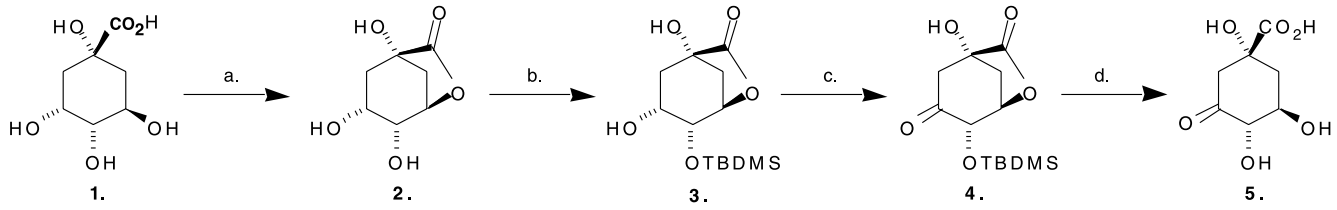

1. 2. 3. 4. 5.

Scheme 1. Synthesis of 3-dehydroquinate. a: 10 mol% *p*TsOH, PhH, reflux (Dean-Stark), 20 h, 86%; b: 1.2 eq. TBDMSCl, 20 mol% 4-DMAP, 15 mol% Et_3N, 6 mol% Bu_4NI, DMF, 90°C, 24 h, 31%; c: 2 eq. (by mass) 3 Å molecular sieves, 2.0 eq. PDC, DCM, 20°C, 5 h, 46%; d: H_2O:AcOH 4:1, 50°C, 48 h, 97%. Full details of the synthesis are given in the Appendix.

sodium phosphate or sodium sulphate. The concentrations of solutions of substrate were calculated on the basis of the limiting change in A_{234} on addition of 1 μg of SCDHQase, taking into account that equilibrium constant for the reaction is 15 [20]. The values of K_m and V_{max} were obtained by fitting the initial rate data to the Michaelis–Menten equation by non-linear regression using Microcal Origin software. Values of k_{cat} were calculated using 16.5, 18.0 and 20.6 kDa for the subunit molecular masses of SCDHQase, MTDHQase and HPDHQase respectively. In the case of MTDHQase and HPDHQase, the kinetic parameters of the His-tagged enzymes were very similar to those previously reported for the corresponding native enzymes [9].

3. Results

3.1. Synthesis of dehydroquinate

The previous synthetic route to 3-dehydroquinate had involved the oxidation of quinic acid by HNO_3 and a lengthy ion exchange chromatographic purification [21]. However, this was unsatisfactory for two reasons: (i) the method leads to formation of both 3- and 5-dehydroquinic acid [22]; the latter may be an inhibitor of dehydroquinase; (ii) the dehydroquinate produced is an off-white to brown solid, even after crystallisation as the ammonium salt; the consequent high background absorbance at 234 nm due to substrate makes detection of low levels of enzyme activity extremely difficult.

Direct lactonisation (Scheme 1, step a), rather than formation of the benzylidene acetal followed by hydrogenolysis under acidic conditions according to the method of Manthey et al. [19], was used for a number of reasons. Firstly, in our hands heating quinic acid with benzaldehyde in acidified toluene led to charring of the reagents within 2 h; this problem was only solved by changing to benzene as solvent. Secondly, the hydrogenolysis step employed by Manthey et al. [19] generally led to poor yields and purification of the lactone by crystallisation from AcOH was found to be extremely unreliable.

In the TBDMS protection (Scheme 1, step b), both temperature and time of reaction appear to be critical. The yield of the desired product is greatly reduced due either to incomplete reaction if the time is too short, or to formation of the bis-silylated compound if the reaction is left longer than 24 h. In the oxidation step (Scheme 1, step c), the use of at least a two-fold excess of freshly activated, powdered, 3 Å molecular sieves is critical. If insufficient sieves are present, the reaction will not go to completion, no matter how large an excess of PDC is used.

3.2. Effects of anions on the kinetic properties of DHQase

The effects of phosphate and sulphate on the kinetic properties of DHQase are shown in Table 2 and Fig. 1. The polyanions both behave as simple competitive inhibitors with respect to 3-dehydroquinate for SCDHQase and HPDHQase as has been previously seen in the case of phosphate with respect to the *A. nidulans* enzyme [2]. By contrast, in the case of MTDHQase, the effects of the anions were more complex. Although sulphate did not change the V_{max}, and thus appeared to act as a competitive inhibitor (data not shown), the dependence of the K_m on the anion concentration did not follow the expected linear model for simple competitive inhibition. In the presence of phosphate, both V_{max} and K_m were increased (Fig. 1C). These results indicate that the anions may bind to more than one site in MTDHQase, leading to multiple effects on the kinetic properties of the enzyme.

3.3. Crystal structure of MTDHQase in complex with sulphate

The monomer fold is essentially identical to the apo-MTDHQase structure reported previously [5], with an average RMSD between the structures of 0.24 Å over all atoms. In the higher resolution structure of the MTDHQase plus sulphate the first and last residues (Leu3 and His143) are flipped 180° in conformation, and electron density was present to permit the inclusion of residues 144–146 in the structure relative to the apoenzyme structure. The catalytically important lid domain is disordered as in the apoenzyme structure, with no interpretable electron density visible between residues 19 and 26. In the sulphate complex, however, the side chain of Arg19 is visible and is positioned in the active site of the enzyme (Fig. 2). Four sulphate molecules were identified in the structure, with two lying in the active site pocket. The first of these (S1) is positioned in the carboxylate binding site as identified

Table 2
Kinetic properties of type II DHQases

Enzyme	K_m (μM)	k_{cat} (s^{-1})	K_i (phosphate) (mM)	K_i (sulphate) (mM)
SCDHQase	100	124	7	11
MTDHQase	24	5.2	[a]	[b]
HPDHQase	205	0.9	9	9

Kinetic parameters were determined as indicated in Section 2. The errors in K_m and k_{cat} are less than 10% of the stated values. The errors in the K_i values are estimated to be ±15% of the stated values.
Assays were performed in 50 mM Tris-acetate buffer, pH 7.0, at 25°C.
[a]In the presence of phosphate, a complex pattern is observed in which V_{max} and K_m are both raised (see Fig. 1).
[b]In the presence of sulphate, the V_{max} remains essentially unchanged, but the dependence of K_m on sulphate concentration is markedly non-linear, indicating that the anion may bind to multiple sites on the enzyme.

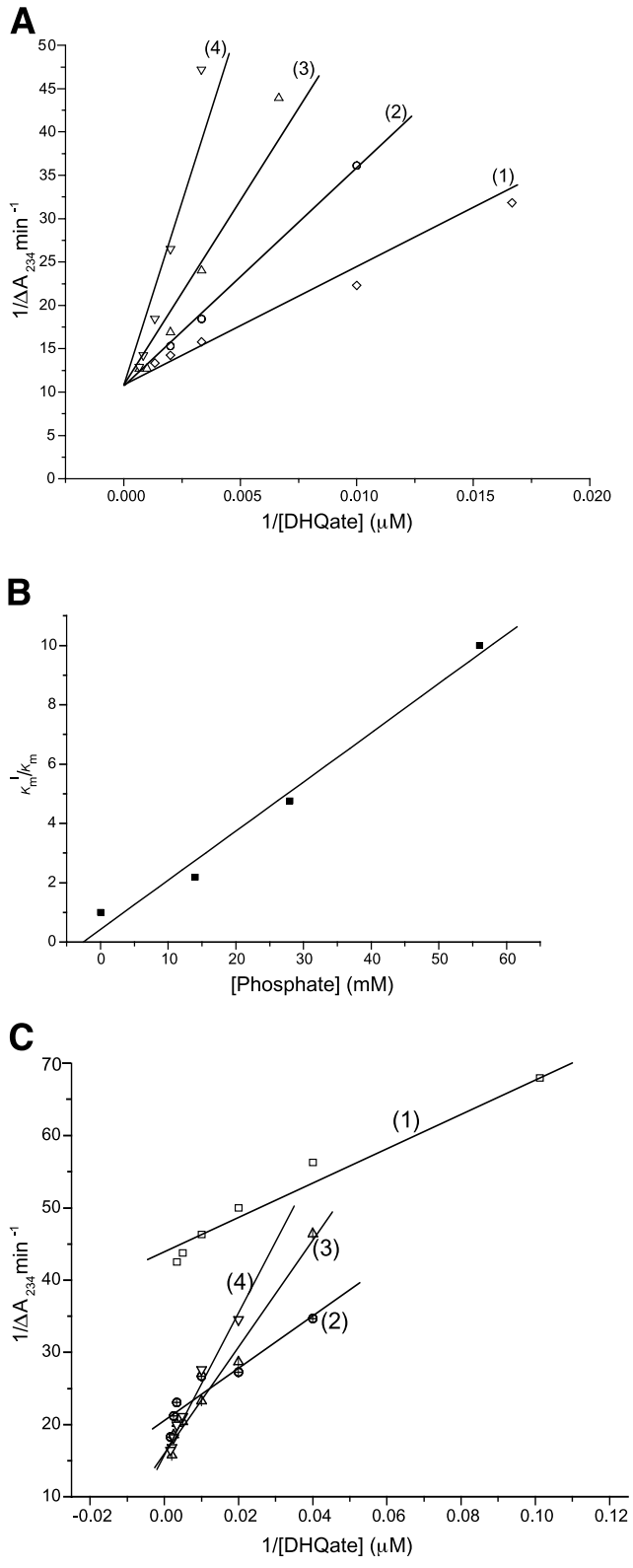

Fig. 1. Inhibition of DHQase by phosphate. A: Lineweaver–Burk plot for inhibition of SCDHQase by phosphate. Lines 1, 2, 3 and 4 refer to 0, 14, 28 and 56 mM phosphate respectively. B: Ratio of K_m^I/K_m vs [phosphate], where K_m and K_m^I are the Michaelis constants for 3-dehydroquinate in the absence and presence of phosphate respectively. For simple competitive inhibition, the slope of this line = $1/K_i$. C: Lineweaver–Burk plot for the effect of phosphate on MTDHQase. Lines 1, 2, 3 and 4 refer to 0, 24, 70 and 140 mM phosphate respectively.

from the SCDHQase–inhibitor complexes [7]. The interactions between the sulphate and Ser107 induce a small hinged movement in the region of the 3_{10} helices H2 and H3 (residues 107–115), to bring it towards the active site. The second sulphate (S2) interacts with the amide nitrogens of the first few residues (17–19) of the lid domain, and with the side chain of Arg19, changing the conformation of this region compared to the apoenzyme. Of the sulphates not in the active site, one (S3) lies on the crystallographic three-fold axes with occupancy 1/3, as is also seen in the SCDHQase structure. The other sulphate (S4) interacts with the side chain of Arg50 from strand β2 and NE1 of Trp61 and NE2 of Gln64 side chains from helix α2.

4. Discussion

The crystal structures of SCDHQase and MTDHQase complexed with phosphate and sulphate respectively were compared in order to try and interpret the effects of these polyanions on the kinetic parameters of the enzymes. From the overlay of the Cα traces of the two structures (Fig. 2) it can be seen that the protein folds overlie well with a backbone RMSD between the structures of 0.98 Å calculated using LSQKAB [18]. The presence of two sulphates in the active site of MTDHQase in comparison with the single phosphate in SCDHQase is consistent with the more complicated kinetics seen in the former enzyme. What is surprising is that the single phosphate bound to SCDHQase does not correspond to either of the sulphates bound in the active site of MTDHQase. This finding could be interpreted structurally as the result of the differences between the two ligands. Both anions have a negative charge of two but at pH 8.5 the phosphate ion has a protonated oxygen (hydroxyl) while sulphate does not. Therefore the protonated oxygen of the phosphate could bind in the analogous position to the C1 hydroxyl of the substrate while this conformation would not be as favourable for sulphate. However, the structure of the SCDHQase–sulphate complex has been solved at 2.8 Å resolution and the anion occupies exactly the same position as is observed in the higher resolution phosphate structure [7].

A comparison of the active sites of the two DHQases is shown in Fig. 3. If we first consider the structure of SCDHQase (Fig. 3A), the phosphate ion forms six hydrogen bonds; with ND1 of His106, ND2 of Asn79, OH of Tyr28, OG of Ser108 and the amide nitrogens of Ile107 and Ser108. The phosphate occupies a position analogous to the carboxylate and C1 hydroxyl of the substrate, with Tyr28 closing the active site lid over the anion. Sequence alignments of type II DHQases show that the H-X-S/T-N motif (residues 106–109), where X is generally a small aliphatic residue, is strongly conserved and essential for substrate recognition of the hydroxyl and carboxylate at C1. In the structure of MTDHQase (Fig. 3B), the S1 sulphate is located in this region, but adopts a different conformation from the P1 phosphate seen in the *S. coelicolor* enzyme. Hydrogen bonds with the OG of Ser103, the ND2 of Asn75 and backbone NH groups of the Ser103 and Ile102 are conserved. These represent the common position of two of the oxygens of the phosphate anion. However, His101 hydrogen bonds to a water molecule rather than the sulphate, and the catalytically important tyrosine in the lid domain does not close over the active site and interact with the sulphate. Instead Arg19 has moved much further into the

Fig. 2. Stereoviews of an overlay of the Ca backbone trace of MTDHQase (black)+sulphate anions (labelled S1–S4) and SCDHQase (grey)+ phosphate anion (labelled P1). The figure was produced using SETOR [23].

active site than observed in the SCDHQase structures, and is able to form a hydrogen bond with the sulphate. The second sulphate ion also interacts with this arginine and also with residues at the N-terminal end of the flexible lid domain.

Therefore, we can account for the more complicated kinetics seen in MTDHQase in the presence of sulphate and phosphate. It is clear that sulphate and presumably phosphate do not occupy exactly the same position as the C1 hydroxyl and carboxylate of the substrate as seen in the *S. coelicolor* enzyme. Therefore we would expect that inhibition would not be as strong as that seen in the *S. coelicolor* enzyme. The presence of a second sulphate interacting with residues in part of the lid domain, in particular Arg19, a residue already shown to be important for catalysis [8], may help to explain the increase in V_{max} seen in the presence of phosphate. This would suggest that ordering or modification of the conformation of residues in the lid domain of MTDHQase is important for increased catalytic activity.

The finding that the sulphate anion does not occupy the same position as the C1 hydroxyl and carboxylate of the substrate helps to explain differences in the inhibition of type II DHQases. A number of selective inhibitors have been synthesised by Frederickson et al. [12] including 2,3-quinic acid and the transition state analogue 2,3-anhydroquinic acid. These inhibitors contain all the structural features of the substrate and transition state respectively, with the exception of the C3 carbonyl which is absent. The K_i values for these inhibitors were two-fold and nine-fold lower respectively for SCDHQase than for MTDHQase. This suggests that while recognition of the C1 carboxylate and hydroxyl is necessary for the specific binding of substrate to SCDHQase, the C3 carbonyl is more important for substrate binding by MTDHQase, quite possibly by interacting with Arg19.

Acknowledgements: We wish to thank the Royal Society (for the award of a Dorothy Hodgkin Research Fellowship to J.L.M.), and the Wellcome Trust and the Biotechnology and Biological Sciences Research Council for financial support.

Appendix. Supplementary information

Details of the synthetic procedure for 3-dehydroquinate are given below. The numbers of the compounds refer to those in Scheme 1. Standard synthetic and analytical procedures were used throughout. Starting materials and reagents are all commercially available.

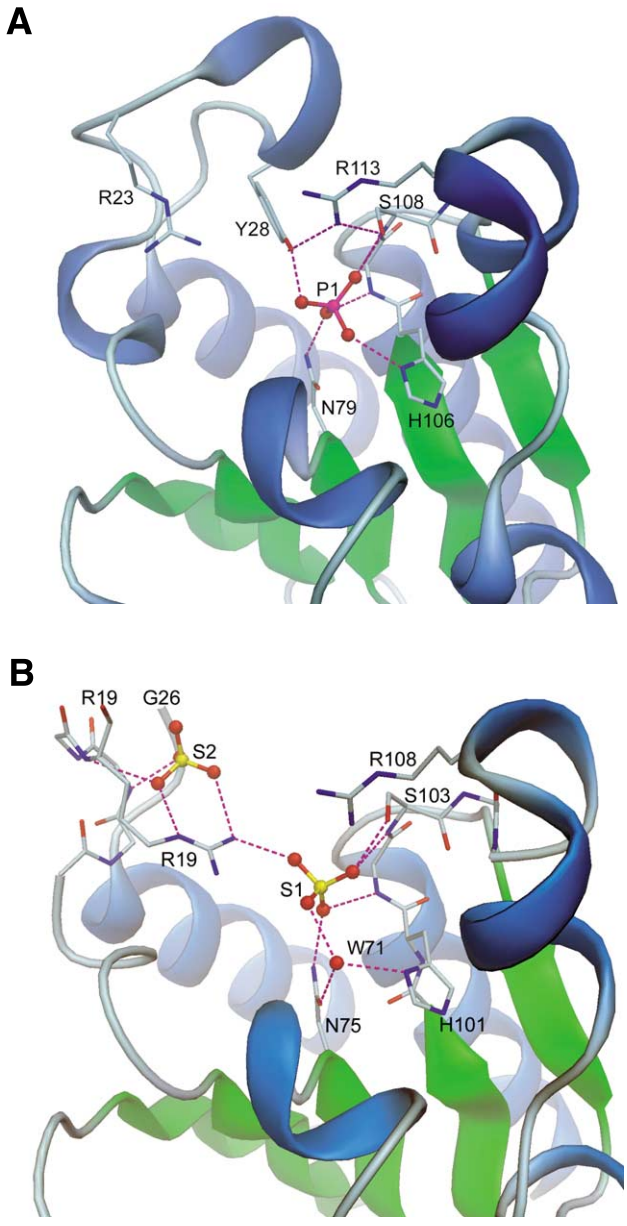

Fig. 3. Ribbon representations of the active sites of (A) SCDHQ with phosphate (P1) bound and (B) MTDHQase with two sulphate ions (S1 and S2) bound. Amino acid residues important for ligand binding are shown in stick and coloured according to atom type, hydrogen bonds are shown as dashed lines coloured magenta. The figure was produced using DINO.

(1*S*,3*R*,4*R*,5*R*)-1,4,5-Trihydroxycyclohexane-1,3-carbolactone 2

Benzene (150 ml) was heated to reflux in a Dean-Stark apparatus for 2 h and allowed to cool to 20°C. Quinic acid **1** (10.0 g, 52.0 mmol) and *p*TsOH (1.0 g, 5.8 mmol) were added and the suspension heated to reflux for 20 h. The benzene was removed under reduced pressure and the residue washed with EtOAc (200 ml). The EtOAc was removed by filtration and the residue dried under high vacuum to give a yellow solid (8.75 g). NMR analysis showed that the crude material **2** (7.8 g, 44.8 mmol, 86%) could be used without further purification. δ_H(400 MHz; CD_3OD) 4.90 (3H, s, 3×OH), 4.74 (1H, dd, *J* 5.1), 4.02 (1H, t, *J* 4.6), 3.74 (1H, ddd, *J* 11.4, 6.6 and 4.5), 2.55 (1H, d, *J* 11.4), 2.26 (1H, ddd, *J* 11.4, 6.0 and 2.9), 2.07 (1H, dddd, *J* 11.8, 6.6, 3.0 and 0.5), 1.91 (1H, t, *J* 11.6); δ_C(100 MHz; CD_3OD) 179.87 (CO_2), 78.27 (CH), 73.50 (*C*[OH]CO_2), 67.73 (CHOH), 67.23 (CHOH), 40.50 (CH_2), 38.23 (CH_2); *m*/*z* (isobutane CI^+) 175.08 ([M+H^+], 100%), 157.07 (9%), 139.07 (8%), 111.07 (11%), 79.02 (10%).

(1*S*,3*R*,4*R*,5*R*)-4-*tert*-Butyldimethylsiloxy-1,5-dihydroxycyclohexane-1,3-carbolactone 3

The lactone **2** (3.76 g, 21.6 mmol) was dissolved in dry DMF (40 ml). TBDMSCl (3.60 g, 23.9 mmol), 4-DMAP (0.50 g, 4.1 mmol), Et_3N (3.6 ml, 25.8 mmol) and Bu_4NI (0.37 g, 1.0 mmol) were added sequentially and the solution was heated to 90°C under N_2. After 24 h the reaction was allowed to cool to 20°C, diluted with EtOAc (200 ml) and filtered (celite). The resulting solution was washed with 1 M HCl (200 ml) and brine (2×200 ml), dried ($MgSO_4$) filtered and evaporated to give the crude product (6.83 g). Silica gel column chromatography (dichloromethane and 2–10% acetone; gradient) was used for initial purification. Repeated crystallisation (Et_2O/petrol) gave the desired product **3** as white crystals (1.81 g, 6.28 mmol, 29%). m.p. 148–152°C (lit. 154–155°C [19]); δ_H(400 MHz; $CDCl_3$) 4.68 (1H, dd, *J* 5.7 and 5.1), 4.11 (1H, t, *J* 4.6), 3.82 (1H, ddt, *J* 11.3, 6.6, 4.5), 2.80 (1H, s), 2.53 (1H, d, *J* 11.5), 2.30 (1H, ddd, *J* 11.4, 6.1 and 3.0), 2.18 (1H, ddd, *J* 12.0, 6.6 and 3.0), 2.09 (1H, d, *J* 11.3), 1.85 (1H, t, *J* 11.6), 0.95 [9H, s, $SiC(CH_3)_3$], 0.17 (3H, s, $SiCH_3$), 0.14 (3H, s, $SiCH_3$); δ_C(100 MHz; $CDCl_3$) 178.04 (CO_2), 76.88 (CH), 72.32 [*C*(OH)CO_2], 67.14 (CH), 66.49 (CH), 41.02 (CH_2), 36.77 (CH_2), 26.07 [$SiC(CH_3)_3$], 18.39 (Si*C*Me_3), −4.19 (Si*C*H_3), −4.48 (Si*C*H_3); *m*/*z* (isobutane CI^+) 289.2 ([M+H^+], 100%), 231.1 (25%), 213.1 (12%), 185.1 (20%), 169.1 (7%), 157.1 (8%), 145.1 (5%), 111.0 (5%), 85.0 (10%), 75.8 (13%).

(1*S*,3*R*,4*R*,5*R*)-4-*tert*-Butyldimethylsiloxy-1-hydroxy-5-oxocyclohexane-1,3-carbolactone 4

3 Å molecular sieves (2.0 g) were heated under high vacuum for 10 min and allowed to cool to 20°C. Dry dichloromethane (20 ml), PDC (2.5 g, 6.65 mmol) and the protected lactone **3** (0.90 g, 3.12 mmol) were added and the suspension stirred under N_2 at 20°C. After 5 h no further change in TLC was visible and the mixture was diluted with Et_2O (150 ml) and filtered (celite). The resulting solution was washed with 1 M HCl (150 ml) and brine (2×150 ml), dried ($MgSO_4$), filtered and evaporated to give the crude product. A flash column (2×6 cm silica, 400 ml Et_2O) gave a white solid in a yellow oil (0.75 g). Crystallisation (petrol) yielded the desired protected 3-dehydroquinic acid (**4**) as fine white needle-shaped crystals (0.41 g, 1.45 mmol, 46%) m.p. 93–94°C, (lit. 92–93°C [19]); δ_H(400 MHz; $CDCl_3$) 4.71 (1H, dd, *J* 6.2 and 3.9), 3.99 (1H, d, *J* 3.7), 3.23 (1H, s), 3.03 (1H, d, *J* 17.1), 2.79 (1H, d, *J* 12.2), 2.74 (1H, dd, *J* 17.1 and 2.4), 2.61 (1H, ddd, *J* 12.1, 6.1 and 2.8), 0.89 [9H, s, $SiC(CH_3)_3$], 0.16 (3H, s, $SiCH_3$), 0.11 (3H, s, $SiCH_3$); δ_C(100 MHz; $CDCl_3$) 203.17 (CO), 177.51 (CO_2), 75.47 (CH), 71.81 [*C*(OH)CO_2], 71.26 (CH), 50.36 (CH_2), 36.20 (CH_2), 25.91 [$SiC(CH_3)_3$], 18.42 (Si*C*Me_3), −4.49 (Si*C*H_3), −4.85 (Si*C*H_3); *m*/*z* (isobutane CI^+) 287.1 ([M+H^+], 100%), 269.1 (10%), 241.1 (8%), 229.1 (85%), 201.1 (10%), 157.1 (30%), 129.1 (7%), 75.0 (10%).

(1*S*,3*R*,4*R*,5*R*)-1,4-Hydroxy-5-oxocyclohexane-carboxylic acid (3-dehydroquinic acid) 5

The protected compound **4** (1.73 g, 6.0 mmol) was dissolved in water (40 ml) and acetic acid (10 ml) and heated to 50°C.

After 48 h the solution was cooled to 20°C and the solvent removed by freeze-drying overnight. The crude material was dissolved in H_2O (200 ml) and washed with EtOAc (2×200 ml). The water was removed by freeze-drying overnight. The washing and freeze drying was repeated to finally give 3-dehydroquinic acid **5** as a white solid/glass (1.04 g, 5.47 mmol, 91%). δ_H(400 MHz; D_2O) 4.12 (1H, dd, *J* 9.5 and 0.6), 3.75 (1H, dt, *J* 9.4 and 7.1), 2.99 (1H, dd, *J* 14.4 and 0.7), 2.42 (1H, dt, *J* 14.3 and 1.6), 2.17–2.14 (2H, m); δ_C(100 MHz; D_2O) 208.44 (CO), 176.79 (CO_2), 80.95 (CH), 74.38 (*C*[OH]CO_2), 71.64 (CH), 47.84 (CH_2), 39.86 (CH_2).

References

[1] Giles, N.H., Case, M.E., Baum, J., Geever, R., Huiet, L., Patel, V. and Tyler, B. (1985) Microbiol. Rev. 49, 338–358.
[2] Kleanthous, C., Deka, R., Davis, K., Kelly, S.M., Cooper, A., Harding, S.E., Price, N.C., Hawkins, A.R. and Coggins, J.R. (1992) Biochem. J. 282, 687–695.
[3] Hawkins, A.R., Lamb, H.K., Moore, J.D., Charles, I.G. and Roberts, C.F. (1993) J. Gen. Microbiol. 139, 2891–2899.
[4] Harris, J.M., Gonzalez-Bello, C., Kleanthous, C., Hawkins, A.R., Coggins, J.R. and Abell, C. (1996) Biochem. J. 319, 333–336.
[5] Gourley, D.G., Shrive, A.K., Polikarpov, I., Krell, T., Coggins, J.R., Hawkins, A.R., Isaacs, N.W. and Sawyer, L. (1999) Nature Struct. Biol. 6, 521–525.
[6] Leech, A.P., James, R., Coggins, J.R. and Kleanthous, C. (1995) J. Biol. Chem. 270, 25827–25836.
[7] Roszak, A.W., Robinson, D.A., Krell, T., Hunter, I.S., Frederickson, M., Abell, C., Coggins, J.R. and Lapthorn, A.J. (2002) Structure 10, 493–503.
[8] Krell, T., Horsburgh, M.J., Cooper, A., Kelly, S.M. and Coggins, J.R. (1996) J. Biol. Chem. 271, 24492–24497.
[9] Bottomley, J.R., Clayton, C.L., Chalk, P.A. and Kleanthous, C. (1996) Biochem. J. 319, 559–565.
[10] Moore, J.D., Lamb, H.K., Garbe, T., Servos, S., Dougan, G., Charles, I.G. and Hawkins, A.R. (1992) Biochem. J. 287, 173–181.
[11] Price, N.C., Boam, D.J., Kelly, S.M., Duncan, D., Krell, T., Gourley, D.G., Coggins, J.R., Virden, R. and Hawkins, A.R. (1999) Biochem. J. 338, 195–202.
[12] Frederickson, M., Parker, E.J., Hawkins, A.R., Coggins, J.R. and Abell, C. (1999) J. Org. Chem. 64, 2612–2613.
[13] Garbe, T., Servos, S., Hawkins, A., Dimitriadis, G., Young, D., Dougan, G. and Charles, I. (1991) Mol. Gen. Genet. 228, 385–392.
[14] White, P.J., Young, J., Hunter, I.S., Nimmo, H.G. and Coggins, J.R. (1990) Biochem. J. 265, 735–738.
[15] Otwinowski, Z. and Minor, W. (1997) Methods Enzymol. 276, 307–326.
[16] Navaza, J. (1994) Acta Crystallogr. A50, 157–163.
[17] Murshudov, G.N., Dodson, E.J. and Vagin, A.A. (1996) in: Macromolecular Refinement (Dodson, E., Moore, M. and Bailey, S., Eds.), pp. 93–104, SERC Daresbury Laboratory, Warrington.
[18] CCP4 (1994) Acta Crystallogr. D50, 760–763.
[19] Manthey, M.K., Gonzalez-Bello, C. and Abell, C. (1997) J. Chem. Soc. Perkin Trans. 1, 625–628.
[20] Kleanthous, C., Reilly, M., Cooper, A., Kelly, S., Price, N.C. and Coggins, J.R. (1991) J. Biol. Chem. 266, 10893–10898.
[21] Grewe, R., Haendler, H. and Keller, H. (1966) Biochem. Prep. 11, 21–26.
[22] Despeyroux, P., Baltas, M. and Gorrichon, L. (1997) B. Soc. Chim. Fr. 134, 777–784.
[23] Evans, S.V. (1993) J. Mol. Graphics 11, 134–138.
[24] Cruickshank, D.W.J. (1999) Acta Crystallogr. D55, 583–601.